Quantitative analysis of length-diameter distribution and cross-sectional properties of fibers from three-dimensional tomographic images

Miettinen, Arttu; Joffe, Roberts; Madsen, Bo; Nättinen, Kalle; Nättinen, Kalle

Published in:
Proceedings of the Risø International Symposium on Materials Science

Publication date:
2013

Document Version
Publisher's PDF, also known as Version of record

Proceedings of the 34th Risø International Symposium on Materials Science:
Processing of fibre composites – challenges for maximum materials performance
Editors: B. Madsen, H. Lilholt, Y. Kusano, S. Fæster and B. Ralph
Department of Wind Energy, Risø Campus
Technical University of Denmark, 2013

QUANTITATIVE ANALYSIS OF LENGTH-DIAMETER DISTRIBUTION AND CROSS-SECTIONAL PROPERTIES OF FIBERS FROM THREE-DIMENSIONAL TOMOGRAPHIC IMAGES

Arttu Miettinen[1], Roberts Joffe[2], Bo Madsen[3], Kalle Nättinen[4], Markku Kataja[1]

[1]Department of Physics, University of Jyväskylä, FI-40014, Finland
[2]Luleå University of Technology, Division of Materials Science SE-97187 Luleå, Sweden
[3]Department of Wind Energy, Technical University of Denmark, Risø Campus, P.O. Box 49, DK-4000 Roskilde, Denmark
[4]VTT Technical Research Centre of Finland, Sinitaival 6, P.O. Box 1300, FI-33101 Tampere, Finland

ABSTRACT

A number of rule-of-mixture micromechanical models have been successfully used to predict the mechanical properties of short fiber composites. However, in order to obtain accurate predictions, a detailed description of the internal structure of the material is required. This information is often obtained from optical microscopy of polished cross-sections of a composite. This approach gives accurate yet local results, but a rather large number of optical images have to be processed to achieve a representative description of the morphology of the material. In this work a fully automatic algorithm for estimating the length-diameter distribution of solid or hollow fibers, utilizing three-dimensional X-ray tomographic images, is presented. The method is based on a granulometric approach for fiber length distribution measurement, combined with a novel algorithm that relates cross-sectional fiber properties to fiber length. The work opens up a possibility to assess multivariate distributions of fiber length and diameter, cross-sectional area or other microstructural fiber properties. As an example, the description of the microstructure of different composites with natural fibers is presented, along with verification of the results.

1. INTRODUCTION

Mechanical properties of short fiber composites have been successfully estimated using rule-of-mixtures based models (Madsen, Joffe, Peltola and Nättinen 2011; Neagu, Gamstedt and Berthold 2006; Andersons, Joffe, and Spārniņš 2006). In addition to mechanical properties of constituents, a significant amount of information about the geometrical structure of the material

is required for successful modeling. Part of this information can be measured using traditional methods, e.g. the volume fractions of the constituents, whereas more intricate techniques are required to measure, e.g., the length, diameter and orientation distributions of fibers and their correlations.

In addition to mechanical modeling, information about a composite structure may be used by composite manufacturers. The manufacturing process typically includes multiple steps, e.g. pelletization of fibers, compounding and injection moulding. Each of these potentially affects the geometry of individual fibers, thus rendering useless any measurements done on intact, non-processed fibers (Peltola, Madsen, Joffe and Nättinen, 2011). However, the morphology of the fibers affects the mechanical properties of the final product. Thus, information about the effect of processing on the fiber geometry is of interest and helps in the optimization of the manufacturing steps.

Traditional methods for measuring the microstructural and geometrical parameters of composites are microscopy of polished cross-sections, and dissolution of matrix to leave only fibers. Both of these traditional methods are time-consuming and they may further affect the geometry as large chemical or mechanical forces must be applied to the samples to transform them into analyzable form. Additionally, in the case of short fiber composites, the dissolution process hides information about e.g. fiber orientation and agglomeration.

X-ray microtomography (X-μCT) is a non-invasive technique for obtaining the three-dimensional internal structure of a sample. It is based on taking a large number of X-ray projection images of the sample, from different angles, and using that data to computationally reconstruct the three-dimensional structure. The result of the process is, roughly speaking, a three-dimensional density map of the sample with a typical resolution around 2 μm.

The two phases, fibers and matrix, can be separated in and X-μCT image of a fibrous composite sample. Without loss of generality it can be assumed that the result of the separation process is an image where the value of each voxel is the volume fraction of fiber material in that particular voxel. Then, voxels entirely in the fiber wall and entirely in the matrix are given values 0 and 1, respectively. We will call such an image semi-binarized.

In the present work, image analysis methods to quantify the microstructure of a composite sample are presented, given a three-dimensional semi-binary image as a starting point. Particularly, a method is given to estimate the multivariate distribution of length and cross-sectional properties of fibers. As a side-effect, other microstructural parameters become straightforward to measure, e.g. the fiber orientation distribution, which can be used to calculate the fiber orientation efficiency factor (Krenchel, 1964).

A similar method has previously been presented by Miettinen and Kataja (2011) and by Miettinen, Luengo Hendriks, Chinga-Carrasco, Gamstedt and Kataja (2012) where it has been assumed that the fibers are geometrically similar, i.e., the volume of a single fiber V_1 is proportional to lD^2, where l is fiber length and D is the smallest dimension of the cross-section of the fiber. In this work we relax this assumption, thereby improving the practical usability of the method considerably. Additionally, the method introduced in this work is capable of measuring many geometrical features of a fiber cross-section, not limited to D, e.g., cross-sectional area.

The results are verified using a computer-generated test data from Miettinen et al. (2011). The method is applied to measure the microstructure of flax fiber composites, whose mechanical properties are then estimated by a micromechanical model and compared to measured values.

2. ESTIMATION OF COMPOSITE MICROSTRUCTURE

Let us first represent the three-dimensional semi-binary image as a function $I(x_1, x_2, x_3)$, whose value is the volume fraction of fiber material in that particular point. Let us now approximate the partial derivatives of I with

$$I_i(\vec{p}) = \frac{\partial I(\vec{p})}{\partial x_i} \approx \left(\frac{\partial G(\sigma_s)}{\partial x_i} * I\right)(\vec{p}), \tag{1}$$

where $G(\sigma)$ is a three-dimensional Gaussian function with zero mean and σ variance in all directions, and $*$ denotes convolution operation. The structure tensor is then defined as (Jähne 2004)

$$S_{ij} = G(\sigma_t) * (I_i I_j). \tag{2}$$

To quantify the orientation of cylindrical structures at $\vec{p}$, the eigenvector of $S_{ij}(\vec{p})$ corresponding to the smallest eigenvalue is calculated.

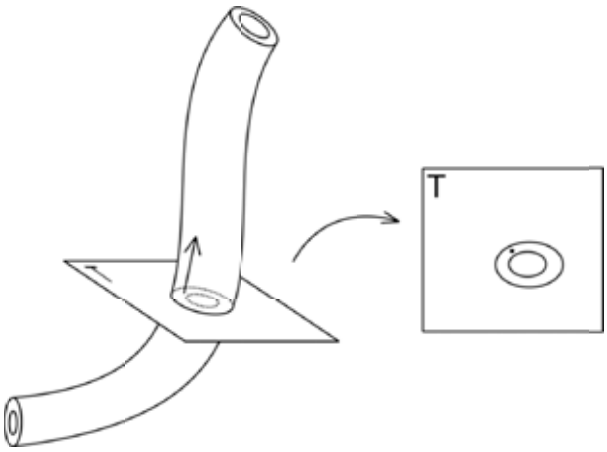

Fig. 1: Slicing a single fiber. The slice T is taken such that its normal (straight arrow) points to the local orientation of the fiber at point $\vec{x}$.

The image I is now sampled uniformly at random locations $\vec{x}_n$, where $n = 1, \ldots, N$ is the index of the location. If $I(\vec{x}_n) < 1$, i.e., the sampled voxel contains matrix material, the point is discarded. Otherwise, a slice around $\vec{x}_n$ is extracted such that the normal of the slice is the local orientation vector, see Fig. 1. The corresponding fiber cross-section is extracted from the slice and desired features are measured; in this work we consider the area of the cross-section A_n and the nominal diameter of the cross-section $d_n = \min(d_{n1}, d_{n2})$, where d_{n1} and d_{n2} are lengths of the projections of the cross-section to the directions of its principal axes. As also other features, in excess of fiber length, can be measured if desired, we denote all of them collectively by ξ_{kn}, where $k = 1, \ldots, K$ indexes a total of K features for the n:th cross-section. See e.g. (Jähne 2004) for a survey on some possible features.

To facilitate calculation of fiber length for the n:th cross-section, we denote by $O(I, l)$ the result of a constrained path-opening operation for image I with length parameter l (Luengo Hendriks

2010). The image $O(I,l)$ thus contains only structures whose longest dimension is less than l. The area of the cross-section corresponding to structures whose length is less than l is then

$$A_n(l) = \int_{A_n} O(I,l)dA, \tag{3}$$

where the integral is taken over the cross-section n. The length distribution of the cross-sectional area is given by

$$\phi_n(l) = \frac{\partial A_n(l)}{\partial l}. \tag{4}$$

We define fiber length L_n as the mode of the length distribution $\phi_n(l)$.

Having now determined the elementary data sets (ξ_{kn}, L_n) for $n = 1, \dots, N$, the sets can be used to create various multivariate distributions of the features ξ_{kn} and L_n. As the probability to sample a fiber is proportional to the volume of the fiber, the resulting distributions will be of type

$$\frac{\partial^{K+1}V}{\partial\xi_1\partial\xi_2\dots\partial\xi_K\partial L}, \tag{5}$$

i.e. (ξ_k, L)-distribution of total fiber volume V.

An interesting side-effect of the above process is that information about the point wise orientation makes it possible to use fiber orientation as one of the features ξ_{kn}. This enables construction of e.g. well-defined fiber orientation distribution. Note that most existing methods give, more or less, the orientation distribution of fiber-matrix interfaces. However, for micromechanical modeling of composites the Krenchel orientation efficiency factor η_o (Krenchel 1964) is more often used. It is defined by

$$\eta_o = \sum_m a_m \cos^4 \alpha_m, \tag{6}$$

where a_m is the ratio between volume of fibers whose orientation direction forms angle α_m with the loading force, and the total volume of all fibers. In the present method, in particular the cross-sectional area A_m and the angle α_m can be selected as measurable features. Approximating that $a_m \approx A_m / \sum_m A_m$ then enables direct application of the definition to approximate the value of η_o.

3. VERIFICATION WITH COMPUTER-GENERATED DATA

As a first test of the method, computer-generated images with a priori known bivariate fiber length and diameter distribution were created, as in (Miettinen et al. 2011). The images were generated using a specific deposition algorithm that modeled the fibers as long rods with small curvature, see Fig. 2 for an example. A total of eight images were generated such that the total number of fibers in them was 1600.

The method in Section 2 was applied to the images and the results were compared to the known distributions, see Fig. 3. The data shows good correspondence between true and measured distributions. The measured length distribution contains more large length values than it should because fibers that are connected to each other form long structures. One should note that in a real composite material there are typically less fiber intersections than in the test structure,

generated by a deposition process where fiber contacts are the only method for the structure to carry its own weight.

Fig. 2: Computer-generated test data. Reproduced from Miettinen and Kataja (2011).

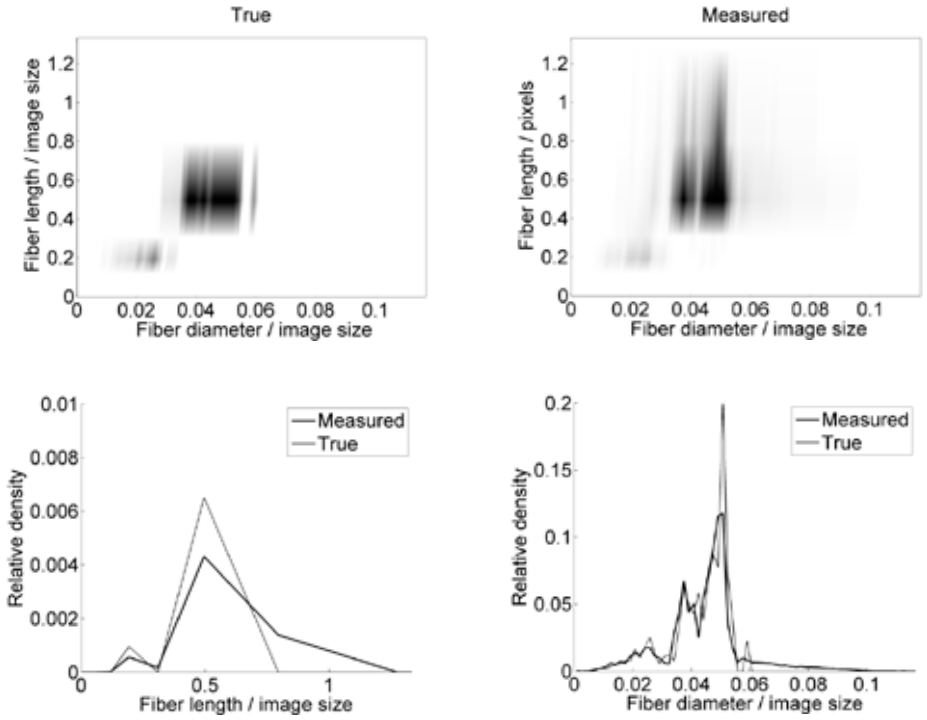

Fig. 3: Comparison between true (top-left) and measured (top-right) distributions of fiber length and diameter, black corresponding to high relative density. Marginal distributions of length (bottom-left) and diameter (bottom-right), with the corresponding true distributions (thin line).

4. APPLICATION TO COMPOSITES

For testing the method, four types of flax fiber composite samples, denoted below by C15, C16, C28 and C29, were manufactured with varying fiber and plasticizer content. The gravimetric composition of these composite samples is given in Table 1. Flax fibers were supplied by Ekotex, Poland. Amylose rich corn starch was supplied by Gargill, USA (Cerestar Amylogel 03003: 65 w-% amylose, 35 w-% amylopectin). The processes of fiber pelletizing, starch acetylation and plasticization are described in more detail in earlier work (Nättinen, Hyvärinen, Joffe and Wallström 2010). The compounding, post processing and injection molding of composite tensile specimens were performed as described earlier, except that in the present work compounds and composites were all compounded with the same temperature gradient from 60 °C in the feeding section to 200 °C in the melting zones and the die.

For X-μCT imaging, cylinders of about 2 mm diameter were cut from the middle part of the tensile specimens. X-μCT images of the samples were taken using an XRadia μCT-400 -device. The pixel size was 1.24 μm, giving a field of view corresponding roughly to the diameter of the cylindrical sample. The images were denoised using variance weighted mean filter and semi-binarized by linear contrast mapping, yielding an image that could be processed as described in Section 2. The results, along with comparison to independently measured values, are given in Table 2. The fiber length distributions and fiber diameter distributions for the four samples are shown in Fig. 4.

Table 1: Gravimetric composition of the flax/PSA composite compounds.

Sample	PSA matrix type	Weight fractions, nominal			Plasticizer content in matrix (w-%)
		Fiber	Starch acetate	Plasticizer	
C15	PSA2.1	0.100	0.720	0.180	20.0
C16	PSA2.1	0.400	0.480	0.120	20.0
C28	PSA5.1	0.100	0.608	0.293	32.5
C29	PSA5.1	0.400	0.405	0.195	32.5

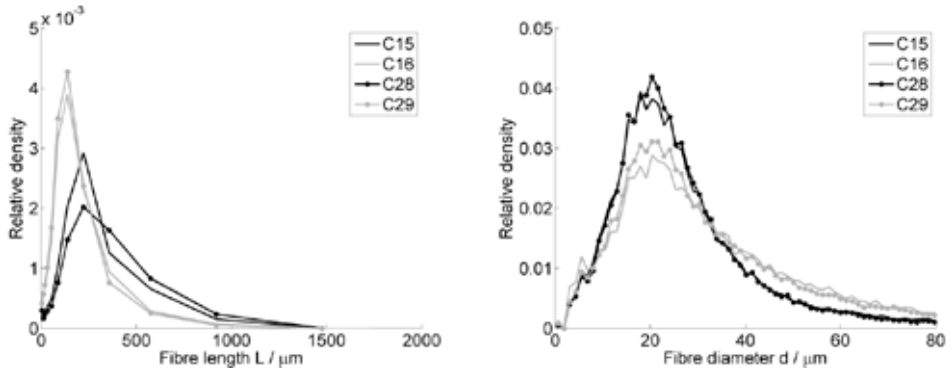

Fig. 4: Fiber length distributions (left) and fiber diameter distributions (right) for the four flax composites obtained using the X-μCT method.

Table 2: Comparison between quantities determined using X-μCT and independent method. Superscript *t* stands for X-μCT method, *g* for gravimetric method, *d* for dissolvement followed by manual microscopic analysis and *m* for value from micromechanical modeling (Nättinen et al. 2010; Madsen et al. 2011). Brackets ⟨·⟩ stand for average value. V_f, V_m and V_v are volume fractions of fibers, matrix and void, respectively. L is fiber length, d is fiber diameter and η_o is Krenchel's orientation efficiency factor.

Sample	V_f^t	V_f^g	V_m^t	V_m^g	V_v^t	V_v^g	$\langle L^t \rangle$	$\langle L^d \rangle$	$\langle d^t \rangle$	$\langle d^d \rangle$	η_o^t	η_o^m
C15	0.11	0.11	0.89	0.89	0	0.00	371±167	347±257	16±10	18±7	0.54	0.61
C16	0.31	0.36	0.69	0.62	0	0.01	262±120	151±105	20±14	19±7	0.73	0.61
C28	0.10	0.09	0.90	0.91	0	0.00	431±196	334±262	16±10	19±7	0.54	0.61
C29	0.27	0.36	0.73	0.64	0	0.01	243±110	293±256	19±13	19±7	0.56	0.61

As mentioned above, the stiffness of short fiber composites with randomly oriented fibers can be predicted with fairly good accuracy by a simple rule-of-mixtures model. The porosity effect can also be easily taken into account. According to (Madsen et al. 2009), the Young's modulus E_c of the composite is thus given by

$$E_c = \left(\eta_o \eta_l V_f E_f + V_m E_m\right)(1 - V_v)^2, \tag{7}$$

where V_f, V_m and V_v are the volume fractions of fibers, matrix and void, and η_o and η_l are the fiber orientation and length efficiency factors, respectively. The stiffness of matrix, E_m, has been measured to be 1.66 GPa for PSA2.1 matrix and 0.45 GPa for PSA5.1 matrix (see also Table 1). The fibers are assumed to be isotropic with E_f = 50 GPa (Lilholt and Lawther 2000). The length efficiency factor η_l is defined as (Cox 1952)

$$\eta_l = 1 - \frac{\tanh(\theta)}{\theta}, \quad \text{where} \quad \theta = 2\frac{\langle L \rangle}{\langle d \rangle}\sqrt{\frac{G_m}{E_f \ln(\frac{\kappa}{V_f})}}. \tag{8}$$

The shear modulus of matrix, G_m, is calculated from the stiffness and Poisson´s ratio ν, assuming an isotropic material with ν = 0.3. Fibers are assumed to be packed hexagonally, thereby implying value of geometrical packing pattern constant $\kappa = \frac{\pi}{2} \cdot \sqrt{3} \approx 0.907$.

The average fiber length $\langle L \rangle$, average fiber diameter $\langle d \rangle$, volume fractions and fiber orientation efficiency factor η_o are obtained from the X-μCT method or the independent measurements, see Table 2. The modeled values of the Young's modulus of the composites are presented in Fig. 5 for either case. Further information about methods used in the independent measurements is found in (Nättinen et al. 2010; Madsen et al. 2011). It must, however, be noted that in the case of independent measurements, the model has been fitted to the experimental data in Fig. 5 using the orientation efficiency factor as a fitting parameter. Such a procedure has been conducted because it is hard to obtain reliable independent measurement for orientation efficiency factor without the X-μCT method.

Based on Table 2, the X-μCT method gives results similar to the independent measurements. However, it must be noted that average fiber diameters $\langle d^t \rangle$ and $\langle d^d \rangle$ are not measured exactly the same way as the fiber cross-section is not perfectly circular. In the manual measurement the fibers are laid down on a microscope slide, so d^d is the diameter of the fiber in an unknown, poorly defined direction. In the X-μCT method, d^t is the diameter of the fiber in such a

direction that the value of d^t is minimal. It is then reasonable to assume that $d^t \lesssim d^d$, a condition that is fulfilled in three cases of four.

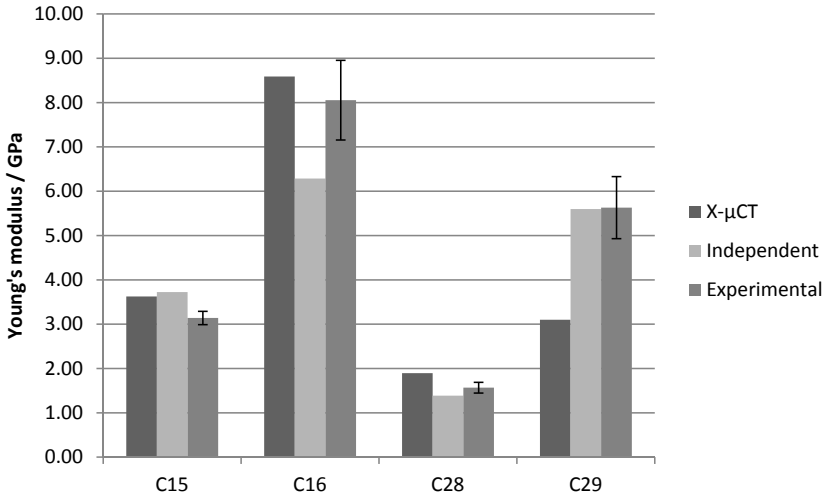

Fig. 5: Comparison between Young's modulus given by the model and tensile test. Bars labeled by 'X-µCT' and 'Independent' are calculated using the model with parameters from X-µCT method or the independent methods, respectively. Bars labeled as 'Experimental' are the results of tensile tests.

5. SUMMARY

Application of the X-µCT method to the computer-generated structure in Section 3 shows good correspondence between true and measured fiber length and diameter distributions. As the test structure contains a lot of fiber intersections, the X-µCT method overestimates the relative number of long fibers. The effect should, however, be much smaller in a real composite sample where there are less fiber intersections.

For real composite samples in Section 4 the X-µCT method gives plausible estimates of the microstructural parameters. Average fiber lengths and diameters measured by the X-µCT method and the independent methods are within one standard deviation from each other.

The modeled and measured stiffness values in Fig. 5 are generally in good agreement, showing the performance of the model, the X-µCT method and the independent measurements. However, it should be noted that X-µCT data fails to predict the Young's modulus of the sample material C29. The difference between volume fractions $|V_f^t - V_f^g|$ is largest in the case of C29, suggesting that the sample for the X-µCT method has been taken from such a location where there are less fibers than on average, thereby hindering effective measurement.

ACKNOWLEDGEMENTS

This work has been partially funded through the Finnish Bioeconomy Cluster FuBio JR2 program.

REFERENCES

Andersons J., Joffe R., Spārniņš E. (2006). Stiffness and strength of flax fiber/polymer matrix composites, Polymer Composites, 27:221-229.

Cox H.L. (1952). The elasticity and strength of paper and other fibrous materials. British Journal of Applied Physics, 3:72-79.

Jähne, B. (2004). Practical handbook on image processing for scientific and technical applications. CRC Press.

Krenchel, H. (1964). Fibre reinforcement. Akademisk forlag. Copenhagen.

Lilholt, H. and Lawther, J.M. (2000). Natural organic fibres. In: Kelly A and Zweben C (eds) Comprehensive composite materials (6 Vols). Vol. 1; Chap. 10. Amsterdam: Elsevier Science, 2000:303–325.

Luengo Hendriks, C.L. (2010). Constrained and Dimensionality-Independent Path Openings. IEEE Trans. Im. Proc. 19, 1587-1595.

Madsen, B., Thygesen A., Lilholt H. (2009). Plant fibre composites – porosity and stiffness, Composite Science and Technology, 69:1057-1069.

Madsen, B., Joffe, R., Peltola, H., Nättinen, K. (2011). Short cellulosic fiber/starch acetate composites - micromechanical modeling of Young's modulus. Journal of Composite Materials, 45 (20): 2119-2131.

Miettinen, A., Kataja M. (2011). Non-destructive analysis of fiber properties using 3D X-ray microtomographic data. Proceedings of the 32nd Risoe International Symposium on Materials Science, Risoe, Denmark, ISBN 978-87-550-3925-4.

Miettinen, A., Luengo Hendriks C.L., Chinga-Carrasco G., Gamstedt E.K., Kataja M. (2012). A non-destructive X-ray microtomography approach for measuring fibre length in short-fibre composites, Comp. Sci. Tech., Volume 72, Issue 15, Pages 1901–1908, http://dx.doi.org/10.1016/j.compscitech.2012.08.008.

Neagu, C., Gamstedt, E.K., Berthold, F. (2006). Stiffness contribution of various wood fibers to composite materials. Journal of Composite Materials. 40: 663-699.

Nättinen, K., Hyvärinen, S., Joffe, R., Wallström, L., Madsen, B. (2010). Naturally compatible: Starch acetate/cellulosic fiber composites. I. Processing and properties *Polymer Composites*, 31(3), 524-535.

Peltola, H., Madsen, B., Joffe, R., Nättinen, K. (2011). The influence of biocomposite processing and composition on natural fiber length, dispersion and orientation Journal of Materials Science and Engineering. Vol. 1 No: 2 , 190-198